Quantitative Analysis of Regional Motion and Thickening by Gated Myocardial Perfusion SPECT: Normal Heterogeneity and Criteria for Abnormality

Tali Sharir, Daniel S. Berman, Parker B. Waechter, Joseph Areeda, Paul B. Kavanagh, Jim Gerlach, Xingping Kang, and Guido Germano

Departments of Imaging and Medicine, Cedars-Sinai Medical Center, Los Angeles; CSMC Burns and Allen Research Institute, Los Angeles; and Departments of Medicine and Radiological Sciences, University of California Los Angeles School of Medicine, Los Angeles, California

Quantitation of regional myocardial function is valuable in patients with coronary artery disease. This study assessed normal heterogeneity and developed and validated normal limits for quantitative regional motion and thickening by gated myocardial perfusion SPECT. **Methods:** Patients underwent rest ^{201}Tl/exercise ^{99m}Tc-sestamibi gated SPECT. Reference values of motion and thickening for 20 myocardial segments were obtained in 105 patients with <5% likelihood of coronary disease (low-likelihood group). Criteria for abnormality of motion and thickening were defined for each segment, using receiver operator characteristic analysis, in 101 patients with coronary disease (training group). Semiquantitative visual interpretation was used as the gold standard. These criteria were prospectively validated in 100 patients (validation group). Criteria for grading motion and thickening abnormalities by severity levels were also defined and validated. **Results:** Normal thickening decreased substantially along the longitudinal axis of the left ventricle, from 69% ± 13% at the apex to 25% ± 11% at the basal segments, whereas normal motion varied within the same ventricular plane. Validation of the criteria for abnormality yielded high accuracy in the detection of motion abnormalities (sensitivity, 88%; specificity, 92%) and thickening abnormalities (sensitivity, 87%; specificity, 89%). Quantitative motion and thickening segmental scores showed good agreement with visual scores. **Conclusion:** Normal regional myocardial contraction by gated myocardial perfusion SPECT is characterized by a substantial apex-to-base decline in thickening and by circumferential heterogeneity in endocardial motion. The assignment of segment-specific threshold values for defining motion and thickening abnormalities provided reasonably accurate identification and grading of regional myocardial dysfunction.

Key Words: gated SPECT; quantitation; motion; thickening

J Nucl Med 2001; 42:1630–1638

Assessment of regional left ventricular function provides useful diagnostic and prognostic information in patients with coronary artery disease (*1*). Echocardiographic and MR studies have shown that regional endocardial motion and wall thickening can be quantitatively assessed using these techniques (*2–5*). However, neither of these methods provides routine, automated delineation of the endocardial and epicardial borders of the myocardium or identification of abnormal function based on region-specific thresholds for abnormality.

We have recently developed a completely automated, quantitative algorithm for the measurement of regional motion and thickening from 3-dimensional gated myocardial perfusion SPECT (*6*). Quantitative measurements by this algorithm correlated with semiquantitative visual interpretation. In contrast to echocardiography and MRI, which determine segmental thickening from direct measurement of myocardial wall thickness, gated myocardial perfusion SPECT provides information on systolic thickening indirectly, using the systolic increase in count density caused by the partial-volume effect (*7*). Because regional end-diastolic thickness of the myocardium is nonuniform (*4,8*), this method might be associated with a characteristic regional heterogeneity in the measurement of thickening, which is not seen by other imaging modalities.

Gated SPECT acquisition of ^{99m}Tc-sestamibi after exercise, injected at peak stress, provides information on peak stress perfusion, coupled with myocardial function at the time of acquisition. Ventricular function assessed during the first hour after stress incorporates baseline information as well as information on poststress cardiac function. Johnson et al. (*9*) showed that patients with reversible stress perfusion defects frequently had poststress stunning. We recently reported (*10*) that postexercise regional motion abnormality detected by gated ^{99m}Tc-sestamibi SPECT is an accurate marker of severe and extensive coronary disease and pro-

Received Sep. 29, 2000; revision accepted Mar. 5, 2001.

For correspondence or reprints contact: Guido Germano, PhD, 8700 Beverly Blvd., Room A047N, Los Angeles, CA 90048.

vides incremental diagnostic information over perfusion alone. To date, however, this approach has been dependent on expert analysis.

The aim of this study was to assess the normal heterogeneity in poststress motion and thickening by ^{99m}Tc gated myocardial perfusion SPECT and to determine and validate quantitative criteria for abnormal poststress motion and thickening for individual myocardial segments.

METHODS

Patient Populations

Reference values of motion and thickening were obtained in 64 consecutive patients with <5% prescan likelihood of coronary artery disease (low-likelihood group), on the basis of Bayesian analysis of age, sex, symptom classification, and electrocardiographic response to exercise (*11*). Patients with atrial fibrillation, left or right bundle branch block, and cardiac pacemaker were excluded.

Criteria for abnormality of motion and thickening were developed in 201 consecutive patients with prescan likelihood of coronary disease ≥5%. Approximately 50% of the patients referred to our nuclear laboratory have low prescan likelihood of coronary disease, the majority of whom have normal perfusion and normal left ventricular function. To avoid high frequency of normal motion and thickening, we excluded patients with low likelihood of coronary disease from this analysis. These 201 patients were randomly assigned to a training group (n = 101) and a validation group (n = 100).

All patients underwent separate acquisition, rest ^{201}Tl/exercise ^{99m}Tc-sestamibi myocardial perfusion SPECT (*12*), with gating of the poststress ^{99m}Tc-sestamibi images.

Acquisition Protocol

A dose of 111–167 MBq (3–4.5 mCi) ^{201}Tl was injected intravenously at rest, and SPECT imaging was initiated 10 min later, using a 30% window centered over the 68- to 80-keV photopeak and a 20% window over the 167-keV peak. Next, 925–1,480 MBq (25–40 mCi) ^{99m}Tc-sestamibi were injected at peak stress, and 8-frame gated SPECT imaging (100% beat length acceptance window) initiated 15–30 min later, using a 15% window centered over the 140-keV photopeak. Acquisitions were performed using a 2-detector 90° camera (Vertex; ADAC, Milpitas, CA), 3-detector camera (Prism; Picker, Cleveland, OH), or 1-detector camera (Orbiter; Siemens, Hoffman Estates, IL), acquiring 60 or 64 projections over 180° (right anterior oblique 45° to left posterior oblique 45°), low-energy, high-resolution collimation, continuous detector rotation, and 35 or 25 s per projection for ^{201}Tl or ^{99m}Tc-sestamibi, respectively. The 8 electrocardiogram (ECG)-gated projection sets of ^{99m}Tc were filtered using a 2-dimensional Butterworth filter (order, 2.5; cutoff frequency, 0.3 cycle per pixel [pixel size = 0.53–0.64 cm]), and automatically reconstructed into transaxial images, using filtered backprojection with a ramp filter. No attenuation or scatter correction was used.

Exercise Protocol

A symptom-limited treadmill exercise test was performed, using the Bruce protocol. Patients received an injection of ^{99m}Tc-sestamibi at peak stress and exercised at the same level for an additional 60 s and then at 1 level lower for 2 min. Electrocardiographic response was considered positive when horizontal or downsloping ST segment depression of ≥1 mm or upsloping ST depression of ≥1.5 mm 80 ms after the J point was observed, or nondiagnostic when ST/T wave abnormalities were present at baseline ECG. Exercise endpoints were achievement of ≥85% of maximal predicted heart rate or ischemic electrocardiographic response.

Semiquantitative Interpretation of Motion and Thickening

Gated SPECT images were visually scored for motion and thickening, using a 20-segment model of the left ventricle (Fig. 1) (*11*). Five representative slices (3 distal, mid, and basal short-axis slices and 1 vertical and 1 horizontal midventricular long-axis slices) were automatically selected for this purpose. Motion was scored using a gray scale, whereas thickening was scored (based on systolic brightening) using a gray scale and a 10-step color scale. A scale of 0–5 was used for grading wall motion (0 = normal, 1 = mildly hypokinetic, 2 = moderately hypokinetic, 3 = severely hypokinetic, 4 = akinetic, 5 = dyskinetic), and a scale of 0–3 for grading thickening (0 = normal, 1 = mildly reduced, 2 = moderately to severely reduced, 3 = no thickening).

Quantitation Algorithm

The automatic quantitation of regional function was performed using a previously described algorithm (*6*). After segmentation of the left ventricle, 3-dimensional endocardial and epicardial surfaces were determined for gated and ungated datasets. Rule-based criteria were used to derive endocardial and epicardial surfaces in areas of apparent absence of perfusion. Endocardial and epicardial surfaces of the gated images were determined by taking into account both the partial-volume effect and geometric factors. Regional motion was measured as the distance (millimeters) between a given endocardial point at end-diastole and end-systole, perpen-

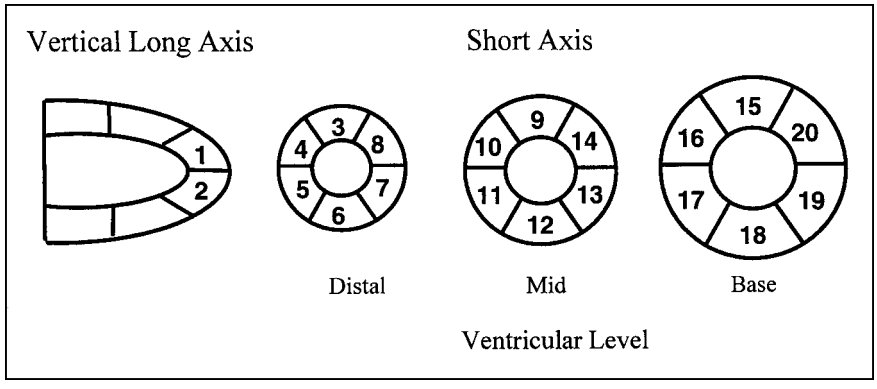

FIGURE 1. Schematic representation of 20-segment model of left ventricle.

dicular to the average midmyocardial surface between end-diastole and end-systole. Myocardial thickening was determined as percentage increase in myocardial thickness (distance between endocardial and epicardial surfaces, normal to the midmyocardial surface) from end-diastole to end-systole.

Criteria for Abnormality of Segmental Motion and Thickening

Reference values (mean ± SD) of motion and thickening of 20 myocardial segments were obtained for the control group. Criteria for abnormality were determined in 101 patients (the training group) with a wide range of poststress motion and thickening abnormalities, using receiver operator characteristic (ROC) analysis for each of the 20 segments, separately. Visual scores were used as a gold standard for the computer-derived measurements, with abnormal motion or thickening defined as a score of ≥2. The diagnostic accuracy of the algorithm, using these thresholds for segmental abnormality was prospectively evaluated in the validation group.

Automatic Segmental Scores

Motion and thickening of 20 myocardial segments were automatically rated using scales analogous to those used for semiquantitative visual scoring, as previously described. Thresholds for these automatic computer scores were iteratively determined for each of the visual categories (0–5 for motion and 0–3 for thickening) to maximize the agreement between visual and automatic scores for each of the segments (*13,14*). The algorithm was developed in the training group and prospectively validated in the validation group by comparing computer-derived and visually determined scores. Summed motion and summed thickening scores were calculated for the automatic as well as for the visual segmental scores.

Statistical Analysis

Reference values of segmental motion and thickening are given as mean ± SD. Longitudinal and circumferential variations in motion and thickening were evaluated using single-factor ANOVA. A probability value of <0.05 was considered significant. For graphic presentation data are shown as mean ± SEM. Differences between patient groups were evaluated using the χ^2 test for categoric variables and unpaired *t* test for continuous variables.

Criteria for abnormality of motion and thickening were obtained using ROC analysis as described previously. Optimal sensitivity and specificity were defined as those yielding the minimal value for $(1 - \text{sensitivity})^2 + 0.95 \times (1 - \text{specificity})^2$. Using these criteria, sensitivity and specificity in detecting segmental motion and thickening abnormality were calculated for each of the 20 myocardial segments in the validation patient subgroup. Threshold criteria for the automatic motion and thickening segmental scores were validated by calculating weighted κ and SE for the automatic scores versus visual scores in the validation group. The relationships between the automatic versus visual summed motion score and the automatic versus visual summed thickening score were evaluated using linear regression analysis.

RESULTS

Baseline Characteristics

Baseline characteristics of the 3 patient subgroups are summarized in Table 1. Compared with the training and validation patient groups, patients with low likelihood of coronary disease were younger, did not have a history of coronary artery disease or typical angina, had less-severe and -extensive perfusion abnormalities at stress and rest, and had a higher left ventricular ejection fraction. There were no statistically significant differences between the training and validation subgroups.

Reference Values of Motion and Thickening

Table 2 shows the heterogeneity in normal motion and thickening observed in the low-likelihood group. Average

TABLE 1
Patient Characteristics

Parameter	Low likelihood (*n* = 64)	Training (*n* = 101)	Validation (*n* = 100)
Age (y)	56 ± 11*†	65 ± 12	64 ± 13
Men	33 (52%)	65 (64%)	63 (63%)
History of myocardial infarction	0 (0%)*†	35 (34.7%)	31 (31%)
History of coronary angioplasty	0 (0%)*†	24 (23.8%)	26 (26%)
History of bypass surgery	0 (0%)*†	10 (9.9%)	12 (12%)
Diabetes mellitus	1 (1.5%)*†	17 (16.8%)	11 (11%)
Hypertension	0 (0%)†	47 (64.5%)	57 (57%)
Typical angina	0 (0%)*†	16 (15.8%)	15 (15%)
Shortness of breath	5 (7.8%)	14 (13.9%)	11 (11%)
Prescan likelihood of CAD	0.02 ± 0.01*†	0.63 ± 0.41	0.60 ± 0.40
Summed stress score	0.3 ± 1.0*†	11 ± 11	9 ± 10
Summed rest score	0 ± 0*†	5 ± 8	4 ± 8
Summed difference score	0.3 ± 1.0*†	6 ± 8	5 ± 6
Ejection fraction (%)	66 ± 8*†	46 ± 17	43_16

*$P < 0.05$ versus training group.
†$P < 0.05$ versus validation group.
CAD = coronary artery disease.

TABLE 2
Reference Values for Segmental Motion and Thickening

Segment	Location	Motion (mm)	Thickening (%)
1	Anteroapical	8.4 ± 1.8	68 ± 14
2	Inferoapical	9.1 ± 1.8	69 ± 13
3	Distal anterior	8.1 ± 1.5	59 ± 13
4	Distal anteroseptal	7.2 ± 1.6	58 ± 13
5	Distal inferoseptal	7.2 ± 1.6	61 ± 12
6	Distal inferior	9.1 ± 1.6	60 ± 13
7	Distal inferolateral	9.5 ± 1.7	60 ± 14
8	Distal anterolateral	9.2 ± 1.7	61 ± 13
9	Mid anterior	8.6 ± 1.4	48 ± 10
10	Mid anteroseptal	6.7 ± 1.6	45 ± 11
11	Mid inferoseptal	5.9 ± 1.6	43 ± 9
12	Mid inferior	7.2 ± 1.3	45 ± 11
13	Mid inferolateral	8.1 ± 1.5	49 ± 12
14	Mid anterolateral	8.3 ± 1.5	48 ± 12
15	Basal anterior	9.0 ± 1.6	23 ± 10
16	Basal anteroseptal	5.9 ± 1.7	23 ± 10
17	Basal inferoseptal	4.8 ± 1.7	20 ± 9
18	Basal inferior	6.6 ± 1.5	22 ± 10
19	Basal inferolateral	8.5 ± 1.6	28 ± 13
20	Basal anterolateral	9.3 ± 1.6	26 ± 12
Average		7.8 ± 2.0	46 ± 20

Data are expressed as mean ± SD; $n = 64$.

values of motion ranged from 4.8 ± 1.7 mm (segment 17, basal inferoseptal) to 9.5 ± 1.7 mm (segment 7, distal inferolateral), whereas average thickening ranged from 20% ± 9% (segment 17) to 69% ± 13% (segment 2, inferoapical). Averaging wall motion and thickening for 4 levels from apex to base (Fig. 2). showed a substantial apex-to-base decrease in thickening, from 68% ± 14% at the apical segments to 24% ± 10% at the basal segments, whereas longitudinal variation in wall motion was small and insignificant. In the 3 ventricular levels along the longitudinal axis (distal, mid, and basal), circumferential motion showed highly significant variations between ventricular walls, with lowest values at the anteroseptal and inferoseptal regions (Fig. 3), whereas circumferential variations in thickening were small, although they were significant at the mid and basal levels (Fig. 4).

Detection of Motion and Thickening Abnormalities

Threshold criteria for the detection of motion and thickening abnormalities at individual myocardial segments, obtained by ROC analysis in the training group, are shown in Figure 5 and are expressed as the number of SDs below the mean reference value of each segment. Most of these cutoff values were 2–3 SDs below the reference value. For most basal segments, the threshold for defining motion and thickening abnormalities was <2 SDs below reference values, reflecting the fact that both visual and quantitative detection of myocardial dysfunction are more complex at the basal regions of the left ventricle.

Figure 6 shows overall sensitivity and specificity in the detection of segments with motion or thickening abnormalities in the validation group. In these 100 patients, visual interpretation detected 579 of 2,000 segments (29%) with motion abnormalities (visual score of ≥2), and 400 segments (20%) with thickening abnormalities (score of ≥2). Using the thresholds for abnormality determined in the training group (Fig. 5), sensitivity and specificity of the quantitative algorithm for the detection of segmental motion abnormality were 88% (510/579) and 92% (1,314/1,421), respectively; for the detection of thickening abnormality, sensitivity and specificity were 87% (349/400) and 89% (1,424/1,598), respectively.

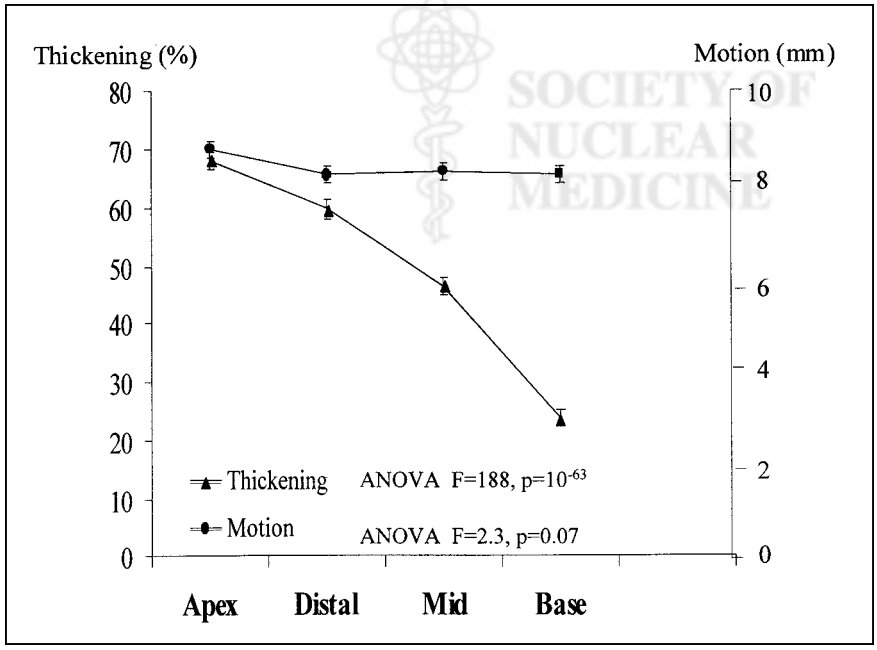

FIGURE 2. Plot of normal motion and thickening (mean ± SEM) at 4 levels from apex to base.

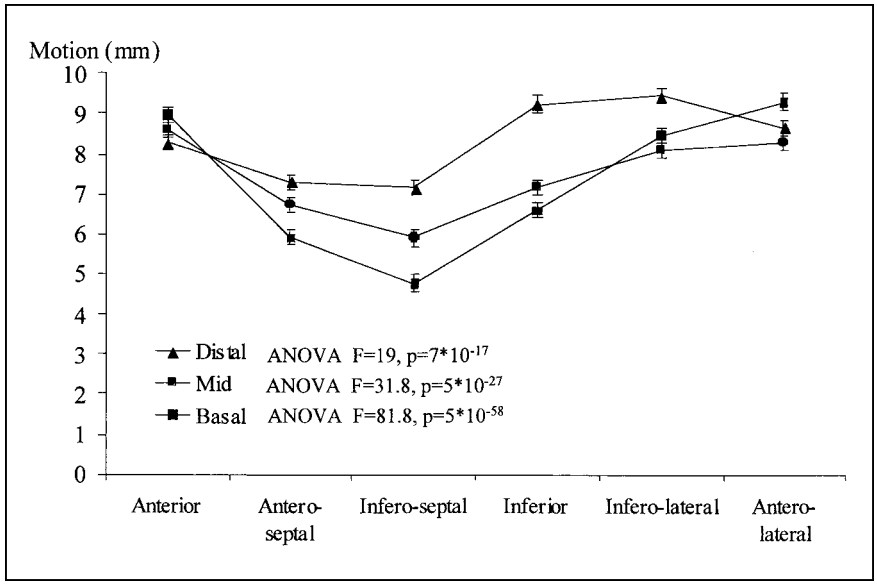

FIGURE 3. Circumferential variations in normal segmental motion at distal, mid, and basal ventricular levels.

The sensitivity and specificity to detect motion and thickening abnormality at each of the 20 segments are shown in Figure 7. Both sensitivity and specificity were >70% in all the segments and >80% in the majority of them. A relatively small number of motion or thickening abnormalities ("positives") in some segments probably accounted for the lower sensitivity observed in those segments.

Automatic Segmental Scores of Motion and Thickening

A comparison between automatically derived segmental scores and visual segmental scores for motion and thickening in the validation group is shown in Tables 3 and 4. The observed (exact) agreement, weighted κ, and SE between the 2 scoring methods were 80%, 0.71, and 0.02 for endocardial motion (Table 3) and 86%, 0.68, and 0.02 for thickening (Table 4), respectively. The relationship between quantitative and visual summed wall motion score and summed thickening score is shown in Figure 8. The automatically derived summed motion scores correlated linearly to the visual summed motion scores ($Y = 0.91X + 3.1$; $r = 0.95$, $P < 0.0001$), and the automatic summed thickening scores correlated linearly to the visual summed thickening scores ($Y = 1.00X + 2.6$; $r = 0.91$, $P < 0.0001$). These relationships showed a slope close to or equal to unity and a small offset, resulting in a nonsignificant difference from the line of identity.

DISCUSSION

This study evaluated the normal heterogeneity of regional motion and thickening by quantitative gated myocardial perfusion SPECT and developed and validated abnormality

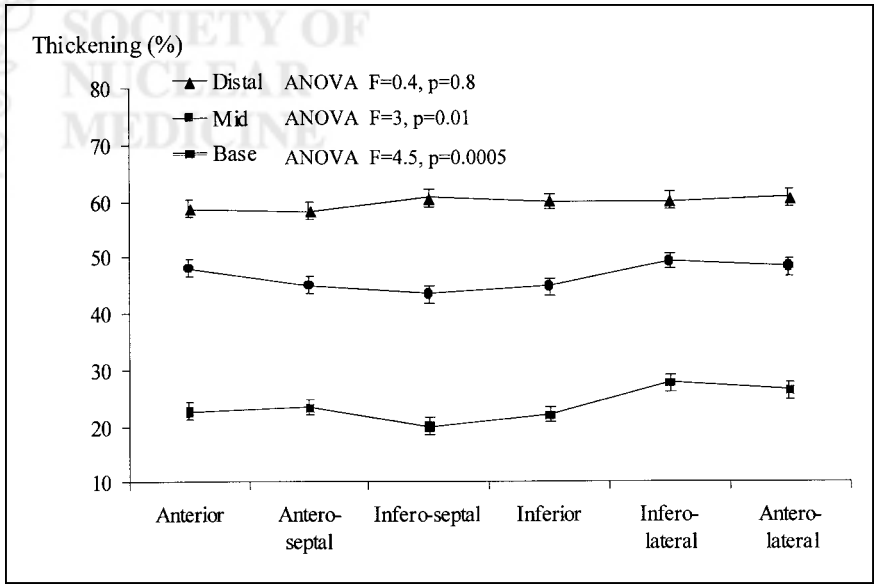

FIGURE 4. Circumferential variations in normal segmental thickening at distal, mid, and basal ventricular levels.

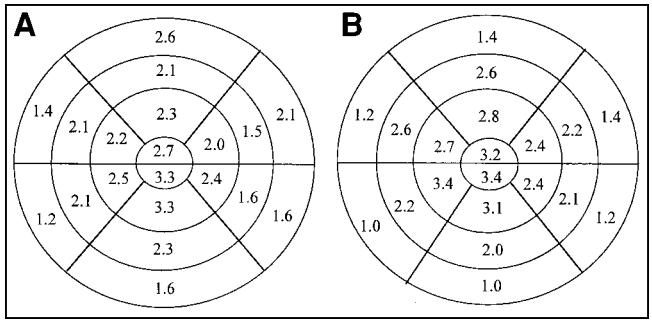

FIGURE 5. Thresholds (number of SDs below reference value) for defining motion (A) and thickening (B) abnormalities.

thresholds for 20 myocardial regions. We found a substantial longitudinal (apex-to-base) variability in systolic thickening, and a considerable circumferential heterogeneity in endocardial motion. However, designation of specific cutoff values of motion and thickening for each of the myocardial regions provided good sensitivity and specificity in the detection of regional myocardial dysfunction.

Quantitative assessment of regional systolic function and the detection of dysfunctional myocardium require definition of "normal" contraction for each myocardial region. Previous studies, using a variety of methods, have shown significant regional differences in normal contraction within the left ventricle (*15–20*). Using echocardiography, Pandian et al. (*17*) revealed substantial differences (range, 30%–70%) in segmental wall thickening between adjacent segments at each ventricular level, as well as between subjects, but similar contraction at different ventricular levels (approximately 50% ± 25%). Using MRI, Sechtem et al. (*19*) showed that normal systolic wall thickening ranged from 35% ± 15% at the inferoseptal segment to 48% ± 28% at the anterolateral segment; however, this difference was insignificant.

In this study, we showed substantial heterogeneity in normal segmental motion and thickening measured by quantitative gated myocardial perfusion SPECT. We found maximal values of thickening at the apical segments, with a progressive decline toward the base. This apex-to-base gradient in thickening has not been described for other imaging modalities. Geometric factors might explain this finding. The normal geometry of the left ventricular wall is characterized by gradual thinning toward the apex (*8*), as verified by measurements of the diastolic wall thickness using MRI (*4*). Because assessment of thickening by gated myocardial perfusion SPECT is based on the count-density–thickness relationship (*7*), which is steeper for smaller thicknesses, thinner parts of the ventricle (such as the distal left ventricle and the apex) show a greater systolic increase in count density, which is translated into higher values of thickening. Endocardial motion, which is less likely to be influenced by the partial-volume effect and myocardial thickness, showed only slight variability between ventricular levels; however, considerable differences in motion were found between segments at the same level, similar to previously described echocardiographic findings, which might be partially explained by the translational motion of the heart (*18*).

The wide range of variability in normal segmental motion and thickening precludes the definition of a single value of these parameters as a lower normal limit. Therefore, we applied ROC analysis to define threshold values for 20 myocardial segments, using semiquantitative visual interpretation as a gold standard. This approach has been previously used in nuclear cardiology for quantitation of relative myocardial perfusion (*14,21,22*); however, to our knowledge, this study is the first to apply this method to quantitative measurements of endocardial motion and wall thickening. This technique is based on the assumptions that visual detection of myocardial dysfunction is accurate and can be used as the gold standard for the quantitative measurements and that absolute values of motion and thickening within a dysfunctional region can be distinguished from interpatient variability of normal myocardial function at that particular region. Our data support the validity of these assumptions. First, most of the threshold values (lower normal limits) for motion and thickening, determined by ROC analysis, were found to be 2–3 SDs below the respective mean normal values, suggesting that <2.5% of normally contracting segments had motion and thickening values below these thresholds. Second, the good sensitivity and specificity of the quantitative measurements in detecting visually defined motion and thickening abnormalities, obtained by applying the normal limits to the validation group, show the adequacy of these thresholds and the comparable diagnostic value of visual and quantitative analysis in the detection of regional myocardial dysfunction.

We showed not only that motion and thickening abnormalities can be effectively detected by the quantitative algorithm but also that they can be automatically graded

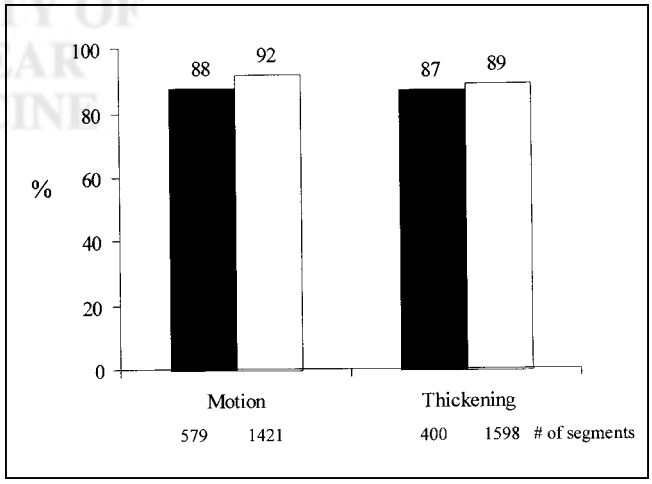

FIGURE 6. Overall sensitivity (black bars) and specificity (white bars) in detecting segmental motion and thickening abnormalities by quantitative algorithm in validation group.

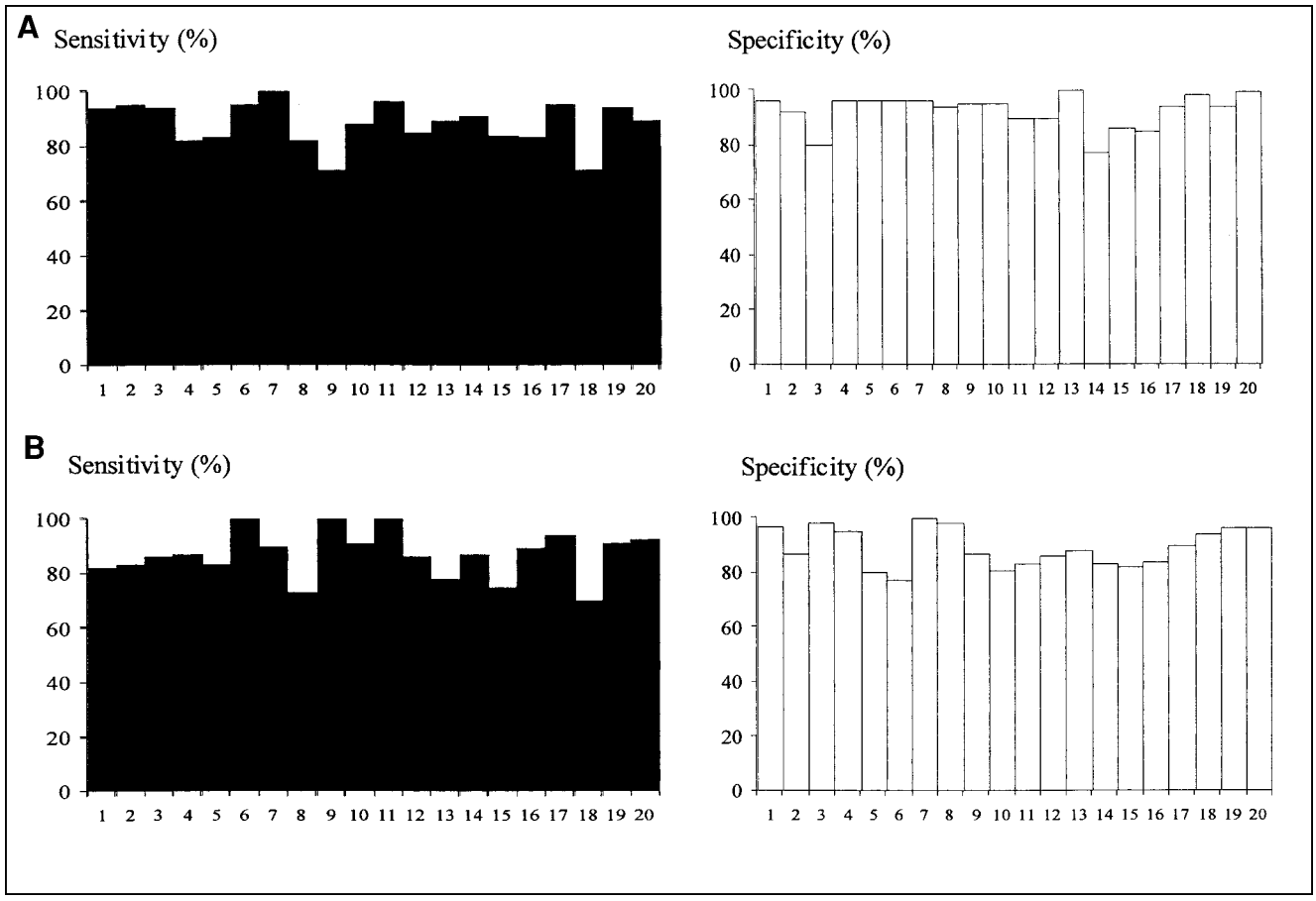

FIGURE 7. Segment-by-segment sensitivity (black bars) and specificity (white bars) in detecting motion (A) and thickening (B) abnormalities by quantitative algorithm in validation group.

into severity levels. Comparison between automatic and visual segmental scores yielded good agreement and κ values (Table 3), and the correlation between automatic summed motion and thickening scores and the respective visual summed scores was highly linear and close to the line of identity (Fig. 8).

We have recently shown that detection of poststress regional myocardial dysfunction in patients with stress-induced ischemia is valuable in identifying severe coronary disease (*10*). The normal limits for regional motion and thickening, defined and validated in this study, have the potential to provide the clinician with a useful, standardized tool for the detection of poststress regional myocardial dysfunction that is not dependent on subjective visual analysis. Grading the severity of regional myocardial dysfunction has diagnostic and prognostic implications in patients with coronary disease. Whereas akinetic segments are less likely to be viable, and hence less likely to improve after

TABLE 3
Correlation Between Automatic and Visual Motion Scores

Automatic scores	Visual scores					Total
	0–1	2	3	4	5	
0–1	**1,314**	60	6	3	0	1,383
2	73	**132**	42	7	2	256
3	27	75	**99**	19	9	229
4	5	11	17	**31**	6	70
5	2	3	6	31	**20**	62
Total	1,421	281	170	91	37	2,000

Agreement = 80%; weighted κ = 0.71; SE = 0.02.
Boldface type indicates segments with exact agreement.

TABLE 4
Correlation Between Automatic and Visual Thickening Scores

Automatic scores	Visual scores			Total
	0–1	2	3	
0–1	**1,426**	48	3	1,477
2	163	**209**	27	401
3	11	31	**82**	127
Total	1,600	288	112	2,000

Agreement = 86%; weighted κ = 0.68; SE = 0.02.
Boldface type indicates segments with exact agreement.

revascularization, hypokinetic segments are more likely to show functional improvement after restoration of coronary flow. Quantitative assessment of regional motion and thickening might be helpful in the follow-up of patients with myocardial dysfunction over time and in evaluating the efficacy of therapeutic interventions, whether medical or invasive, in these patients. In this study, we showed that quantitative grading of the severity of regional myocardial dysfunction, using ^{99m}Tc gated SPECT, is feasible and relatively accurate. Although the current thresholds for abnormality were developed for poststress ^{99m}Tc-sestamibi imaging, we believe that the same thresholds can be applied to resting ^{99m}Tc as well. Future studies will be needed to evaluate this assumption and determine these limits in gated ^{201}Tl SPECT studies.

This study did not validate segmental scores of motion and thickening by gated SPECT against an independent gold standard of myocardial contraction, such as echocardiography or MRI. Our group has previously reported good agreement between gated SPECT and echocardiography for wall motion and thickening scores obtained by visual interpretation (*23*). In this study, visual scores were used as a gold standard for the quantitative measurements, and quantitative thresholds for each of the visual 0–3 severity levels of motion and thickening abnormality were determined. It should be noted that technical problems during the acquisition, which would affect the quality of perfusion or function images, would result in inaccurate interpretation of motion and thickening by both visual and

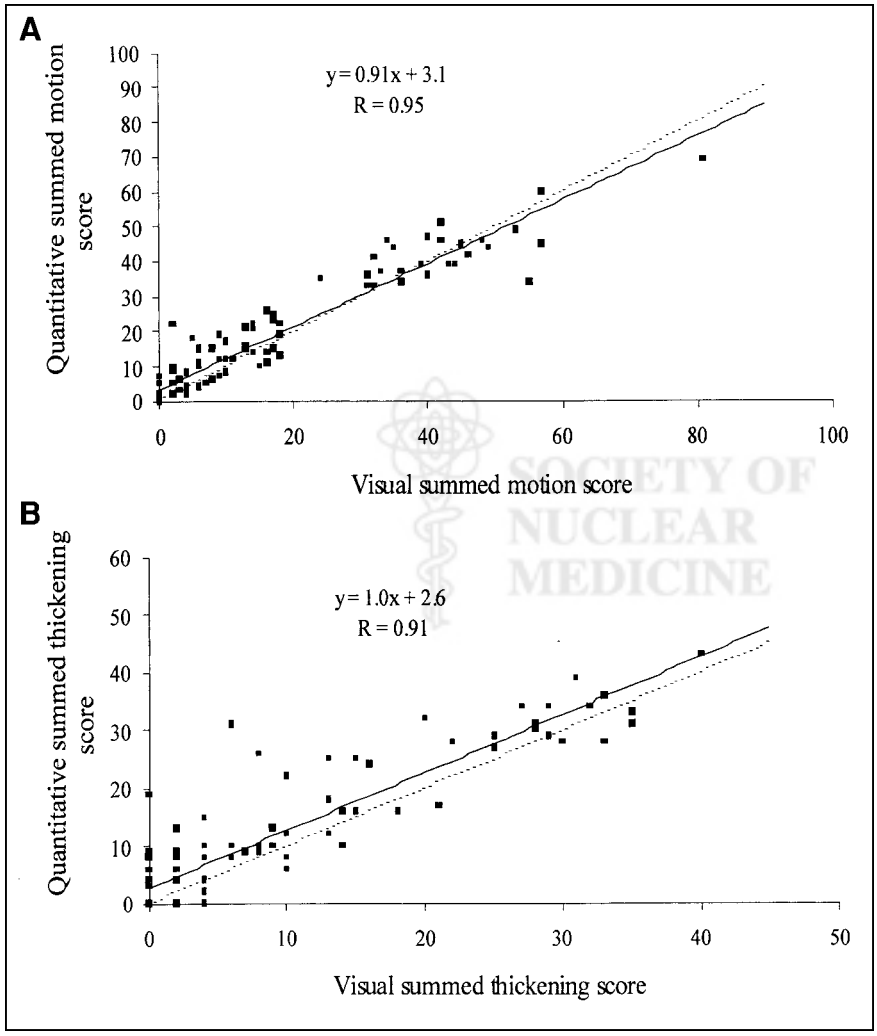

FIGURE 8. Correlation between quantitative versus visual summed motion score (A) and summed thickening score (B). Solid line indicates linear fit and dashed line indicates line of identity.

quantitative methods. These problems include low count scans, gating errors, arrhythmia, and patient motion.

CONCLUSION

This study showed that normal regional myocardial contraction by gated myocardial perfusion SPECT is characterized by a substantial apex-to-base decline in thickening and by circumferential heterogeneity in endocardial motion. The assignment of segment-specific threshold values for defining motion and thickening abnormalities provided relatively accurate identification and grading of regional myocardial dysfunction.

ACKNOWLEDGMENTS

This work was supported in part by National Heart, Lung and Blood Institute, National Institutes of Health, grant RO1 HL57166. The automatic algorithm described in this work is owned by Cedars-Sinai Medical Center, which receives royalties from its licensing. A minority portion of those royalties is shared by the authors.

REFERENCES

1. Shiina A, Tajik AJ, Smith HC, Lengyel M, Seward JB. Prognostic significance of regional wall motion abnormality in patients with prior myocardial infarction: a prospective correlative study of two-dimensional echocardiography and angiography. *Mayo Clin Proc.* 1986;61:254–262.
2. Moynihan PF, Parisi AF, Feldman CL. Quantitative detection of regional left ventricular contraction abnormalities by two-dimensional echocardiography. I. Analysis and methods. *Circulation.* 1981;63:752–760.
3. Parisi AF, Moynihan PF, Feldman CL. Quantitative detection of regional left ventricular contraction abnormalities by two-dimensional echocardiography. II. Accuracy in coronary artery disease. *Circulation.* 1981;63;760–767.
4. Beyar R, Shapiro EP, Graves WL, et al. Quantification and validation of left ventricular wall thickening by a 3-dimensional volume element magnetic resonance imaging approach. *Circulation.* 1990;81:297–307.
5. Holman ER, Buller VG, de Roos A, et al. Detection and quantification of dysfunctional myocardium by magnetic resonance imaging: a new three-dimensional method for quantitative wall thickening analysis. *Circulation.* 1997;95: 924–931.
6. Germano G, Erel J, Lewin H, Kavanagh PB, Berman DS. Automatic quantitation of regional myocardial wall motion and thickening from gated technetium-99m sestamibi myocardial perfusion single-photon emission computed tomography. *J Am Coll Cardiol.* 1997;30:1360–1367.
7. Hoffman EJ, Huang SC, Phelps ME. Quantitation in positron emission computed tomography. 1. Effect of object size. *J Comput Assist Tomogr.* 1979;3:299–308.
8. Streeter DD. Gross morphology and fiber geometry of the heart. In: Berne RM, Sperelakis NS, Geiger SR, eds. *The Heart*. Bethesda, MD: American Physiological Society; 1979:61–112.
9. Johnson LL, Verdesca SA, Aude WY, et al. Postischemic stunning can affect left ventricular ejection fraction and regional wall motion on post-stress gated sestamibi tomograms. *J Am Coll Cardiol.* 1997;30:1641–1648.
10. Sharir T, Bacher-Stier C, Lewin HC, et al. Identification of severe and extensive coronary artery disease by post-exercise regional wall motion abnormalities in Tc-99m sestamibi gated single photon emission computed tomography. *Am J Cardiol.* 2000;86:1171–1648.
11. Diamond GA, Staniloff HM, Forrester JS, Pollock BH, Swan HJ. Computer-assisted diagnosis in the noninvasive evaluation of patients with suspected coronary artery disease. *J Am Coll Cardiol.* 1983;1:444–455.
12. Berman DS, Kiat H, Friedman JD, et al. Separate acquisition rest thallium-201/stress technetium-99m sestamibi dual-isotope myocardial perfusion single-photon emission computed tomography: a clinical validation study. *J Am Coll Cardiol.* 1993;22:1455–1464.
13. Germano G, Kavanagh PB, Waechter PB, et al. A new algorithm for the quantitation of myocardial perfusion SPECT. I. Theoretical aspects. *J Nucl Med.* 2000;41:712–719.
14. Sharir T, Germano G, Waechter PB, et al. A new algorithm for the quantitation of myocardial perfusion SPECT. II. Validation and diagnostic yield. *J Nucl Med.* 2000;41:720–727.
15. LeWinter MM, Kent RS, Kroener JM, Carew TE, Covell JW. Regional differences in myocardial performance in the left ventricle of the dog. *Circ Res.* 1975;37:191–199.
16. Greenbaum RA, Gibson DG. Regional non-uniformity of left ventricular wall movement in man. *Br Heart J.* 1981;45:29–34.
17. Pandian NG, Skorton DJ, Collins SM, Falsetti HL, Burke ER, Kerber RE. Heterogeneity of left ventricular segmental wall thickening and excursion in 2-dimensional echocardiograms of normal human subjects. *Am J Cardiol.* 1983; 51:1667–1673.
18. Weyman AE, Franklin TD, Hogan RD, et al. Importance of temporal heterogeneity in assessing the contraction abnormalities associated with acute myocardial ischemia. *Circulation.* 1984;70:102–112.
19. Sechtem U, Sommerhoff BA, Markiewicz W, White RD, Cheitlin MD, Higgins CB. Regional left ventricular wall thickening by magnetic resonance imaging: evaluation in normal persons and patients with global and regional dysfunction. *Am J Cardiol.* 1987;59:145–151.
20. Waiter GD, McKiddie FI, Redpath TW, Semple SIK, Trent RJ. Determination of normal regional left ventricular function from cine-MR images using a semi-automated edge detection method. *Magn Reson Imaging.* 1999;17:99–107.
21. Maddahi J, Van Train K, Prigent F, et al. Quantitative single photon emission computed thallium-201 tomography for detection and localization of coronary artery diease: optimization and prospective validation of a new technique. *J Am Coll Cardiol.* 1989;14:1689–1699.
22. Van Train KF, Areeda J, Garcia EV, et al. Quantitative same-day rest-stress technetium-99m-sestamibi SPECT: definition and validation of stress normal limits and criteria for abnormality. *J Nucl Med.* 1993;34:1494–1502.
23. Chua T, Kiat H, Germano G, et al. Gated technetium-99m sestamibi for simultaneous assessment of stress myocardial perfusion, postexercise regional ventricular function and myocardial viability: correlation with echocardiography and rest thallium-201 scintigraphy. *J Am Coll Cardiol.* 1994;23:1107–1114.